

# Jones matrix analysis of high-precision displacement measuring interferometers

Peter de Groot

zygo, Laurel Brook Road, Middlefield, CT USA 06455

e-mail: *peterd@zygo.com*

**Abstract – I analyze error sources in high-performance DMI using Jones Calculus. The analysis includes frequency and polarization mixing, and synchronous noise in the heterodyne laser source. The model indicates that an accuracy of 0.1 nm is achievable at high data rates for the next generation of DMI tools.**

## 1 What is DMI?

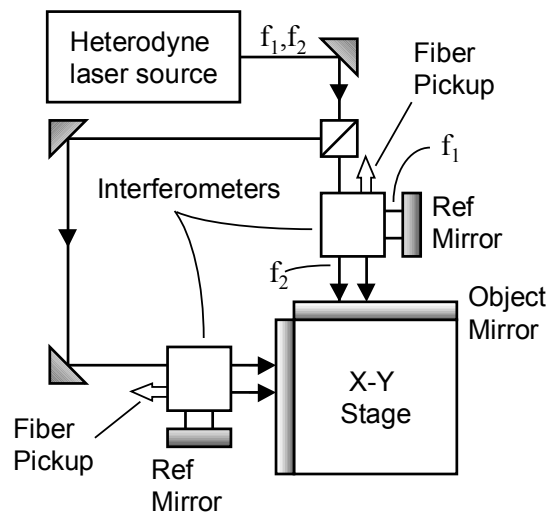


**Figure 1: Heterodyne DMI system for x-y stage metrology.**

Heterodyne displacement-measuring interferometry (DMI) is a high-precision metrology tool based on monochromatic, two-beam interference. It is one of the most widespread applications of optical interferometry in research and manufacturing. DMI is an essential tool for microlithography, e-beam mask writing, scanning electron microscopy, memory repair, and precision machining.

Fig.1 shows a typical DMI geometry for x-y stage metrology. The heterodyne source generates a collimated beam with an optical frequency split  $f_1$ - $f_2$  between the orthogonal polarizations. The frequency split depends on the source type

and can be anywhere from a few MHz (Zeeman split HeNe) to several tens of MHz (acousto-optic modulation). At each interferometer, the polarization states separate and travel to object and reference mirrors. After recombination at a fiber optic pickup, the beams travel to high-speed electronics that interpret the heterodyne signal and report the stage position.<sup>1</sup> Depending on the configuration, DMI can resolve displacements to 0.3 nm at velocities of 2 m/s. Heterodyne systems readily accommodate multiple axes ( $x, y, \theta...$ ), and the technology is continuously improving.

## 2 System modeling

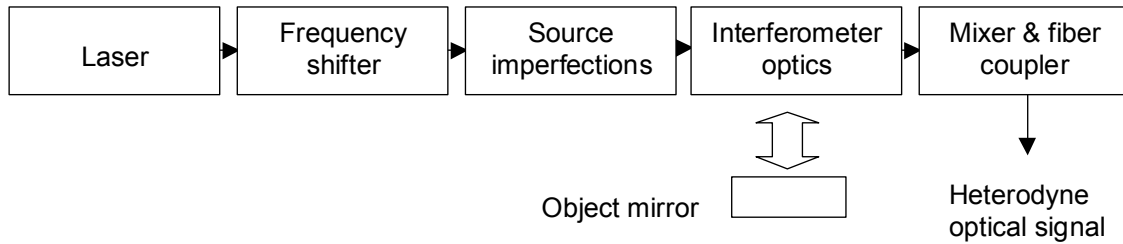


**Figure 2: Functional block diagram of a heterodyne DMI measurement axis.**

Designing a DMI instrument requires detailed modeling of the optical system, starting with a functional block diagram such as is shown in Fig.2. One then applies Jones calculus to represent each of the blocks mathematically for subsequent literal and numerical analysis.<sup>2</sup>

The final product of the optical system is the heterodyne optical signal, given by

$$S = | Mix \cdot Interf \cdot SourceError \cdot Shift \cdot Laser |^2. \quad (1.)$$

The first three terms starting from the right in Eq.(1) relate to the heterodyne laser source pictured in Fig.1. The Jones matrices are:

$$Laser = \frac{1}{\sqrt{2}} \begin{pmatrix} 1 \\ 1 \end{pmatrix} \quad (2.)$$

$$Shift(t) = W(2\pi f t) \quad (3.)$$

$$SourceError [ t ] = align(\delta\alpha_{in}) \cdot orth(\delta\chi) \cdot ellp(\vartheta) \cdot add ( t, N). \quad (4.)$$

The sub matrices and parameters appear in Table 1. The *SourceError* matrix comprises several error sources, from additive noise to polarization misalignment.

Matrix name	Matrix form	Typical values
Polarized phase shift	$W(\delta) = \begin{pmatrix} e^{+i\delta/2} & 0 \\ 0 & e^{-i\delta/2} \end{pmatrix}$	-
Polarization rotation	$rot(\vartheta) = \begin{pmatrix} \cos(\vartheta) & \sin(\vartheta) \\ -\sin(\vartheta) & \cos(\vartheta) \end{pmatrix}$	-
Polarization misalignment	$align(\delta\alpha_{in}) = rot(\delta\alpha_{in})$	$\delta\alpha_{in} = 8 \text{ mrad}$
Polarization orthogonality	$orth(\delta\chi) = \begin{pmatrix} \cos(\delta\chi/2) & -\sin(\delta\chi/2) \\ -\sin(\delta\chi/2) & \cos(\delta\chi/2) \end{pmatrix}$	$\delta\chi = 10 \text{ mrad}$ (40dB)
Polarization ellipticity	$ellip(\vartheta) = W(\pi/2) \cdot rot(\vartheta)$	$\vartheta = 10 \text{ mrad}$ atan(minor/major)
Additive synchronous noise	$add(t, N) = \sqrt{1 + N \cos[2\pi f t]} \cdot I$	$N = 0.5\%$ $f = 20 \text{ MHz}$

Table 1: Heterodyne frequency shifter and source error matrices.

### 3 Interferometer

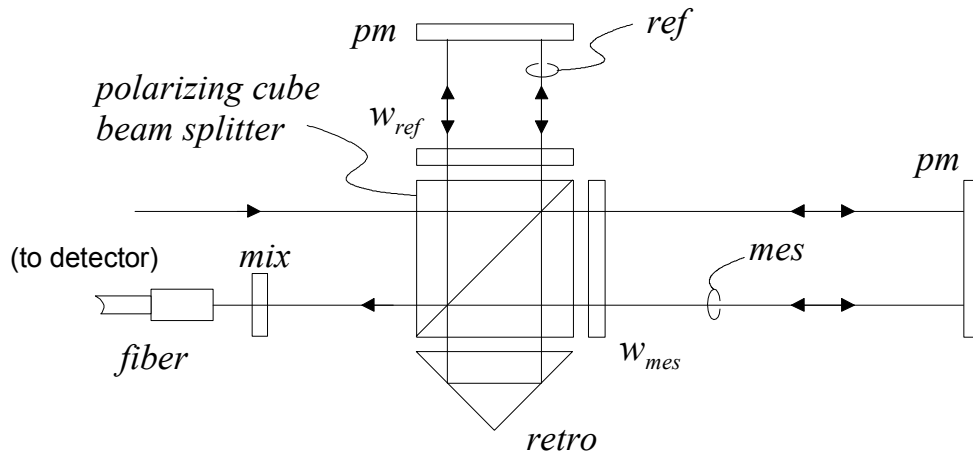


Figure 3: High-stability plane mirror interferometer.

Interferometers for x-y stage metrology use a double pass to the plane mirror to compensate for tip and tilt.<sup>3</sup> The measurement path therefore comprises two paths connected by a corner-cube retroreflector:

$$Mes(x) = mes_2(x) \cdot retro \cdot mes_1(x) \quad (5.)$$

where

$$mes_1(x) = split_R \cdot w_{mes} \cdot U(x) \cdot pm \cdot U(x) \cdot w_{mes} \cdot split_T \quad (6.)$$

$$mes_2(x) = split_T \cdot w_{mes} \cdot U(x) \cdot pm \cdot U(x) \cdot w_{mes} \cdot split_R \quad (7.)$$

and the various sub matrices are cataloged in Table 2. The reference path is

$$Ref = ref_2 \cdot retro \cdot ref_1 \quad (8.)$$

where

$$ref_1 = split_T \cdot w_{ref} \cdot pm \cdot w_{ref} \cdot split_R \quad (9.)$$

$$ref_2 = split_R \cdot w_{ref} \cdot pm \cdot w_{ref} \cdot split_T. \quad (10.)$$

There are additionally unwanted paths, including a possible quadruple pass:

$$Mult(x) = mes_2(x) \cdot [ retro \cdot mes'(x) \cdot retro \cdot mes'(x) ] \cdot retro \cdot mes_1(x) \quad (11.)$$

where

$$mes'(x) = split_R \cdot w_{mes} \cdot U(x) \cdot pm \cdot U(x) \cdot w_{mes} \cdot split_R \quad (12.)$$

the *Mult* matrix is zero for perfect components and alignments. The complete interferometer matrix is

$$Interf(x) = Ref + Mes(x) + Mult(x + \delta x), \quad (13.)$$

where the small offset  $\delta x$  accounts for small path length differences that influence the interference between the *Mes* and *Mult* terms.

The final matrix to complete the model is the fiber coupling to the electronics card, including a polarizer to combine the reference and measurement beams:

$$Mix(\alpha_{mix}) = fiber \cdot P_{mix}(\alpha_{mix}). \quad (14.)$$

Matrix name	Matrix form	Typical values
Polarizer	$P(a, b) = \begin{pmatrix} \sqrt{a} & 0 \\ 0 & \sqrt{b} \end{pmatrix}$	-
Plane mirror at normal incidence	$pm = P(R_m, R_m)$	$R_m = 92\%$
Retroreflector	$retro = \sqrt{R_{retro}} \cdot rot(\zeta)$	$R_{retro} = 80\%$ $\zeta = 85 \text{ mrad}$
Beam propagation	$U(x) = \exp(2\pi i x / \lambda) \cdot I$	$\lambda = 632.8 \text{ nm}$
Anti-reflection coatings	$A = \sqrt{T_A} \cdot I$	$T_A = 99.5\%$
Cube beam splitter reflection	$split_R = A \cdot P(Rc_s, Rc_p) \cdot A$	$Rc_s = 99.9\%$ $Rc_p = 0.1\%$
Cube beam splitter transmission	$split_T = A \cdot P(Tc_s, Tc_p) \cdot A$	$Tc_s = 0.1\%$ $Tc_p = 99.9\%$
Waveplate	$w = A \cdot rot(45^\circ \pm \delta\alpha) \cdot W(\pi/2 \pm \delta\gamma) \cdot rot(-45^\circ \mp \delta\alpha) \cdot A$	$\delta\alpha = 8 \text{ mrad}$ $\delta\gamma = 13 \text{ mrad}$
Mixing polarizer (dichroic)	$P_{mix}(\delta\alpha_{mix}) = rot(45^\circ + \delta\alpha_{mix}) \cdot P(T_{mix}, 0) \cdot rot(-45^\circ - \delta\alpha_{mix})$	$\delta\alpha_{mix} = 10 \text{ mrad}$ $T_{mix} = 80\%$
Fiber coupler	$fiber = \sqrt{T_{fib}} \cdot I$	$T_{fib} = 70\%$

Table 2: Interferometer and fiber coupler matrices.

## 4 Results

One way to take advantage of the modeling is by means of computer simulation, for which the literal math is converted into software functions. Phase estimation algorithms interpret the simulated heterodyne signal, revealing potential errors in the optical system. The example results in Fig.4 show small signal fluctuations and cyclic error related to known component and alignment imperfections.

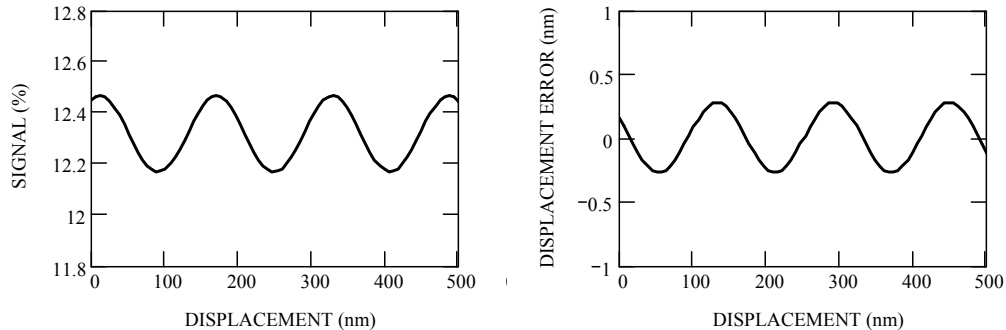


Figure 4: Predicted signal fluctuation (left) and cyclic error (right) in a plane-mirror DMI system.

## 5 Conclusions

There are several additional error sources not discussed in this short paper, including surface reflections and errors that vary with stage angle. All of these errors can and have been incorporated into a more extensive Jones matrix model. These analyses show that commercial DMI systems are presently capable of sub-nm accuracy under most circumstances. A target accuracy of 0.1 nm appears reasonable for new interferometer designs in the next generation of DMI tools.

The Author gratefully acknowledges the insight and contributions of Prof. Henry Hill of the Zetetic Institute, Tucson, AZ to this work. M. Holmes, L. Deck and F. Demarest also made important contributions to this paper.

## REFERENCES AND NOTES

- <sup>1</sup> F. Demarest, "High-resolution, high-speed, low data age uncertainty, heterodyne displacement measuring interferometer electronics," *Meas. Sci. Technol.* Vol. 9, pp.1024–1030, 1998.
- <sup>2</sup> See for example: J. A. Stone and L. P. Howard, "A simple technique for observing periodic nonlinearities in Michelson interferometers," *Prec. Eng.* vol. 22, pp.220-232, 1998, and references therein.

---

<sup>3</sup> S.J. Bennett, "A double-passed Michelson interferometer," *Optics Communications*, vol. 4, 428-430, 1972.